DEPARTMENT OF THE INTERIOR
UNITED STATES GEOLOGICAL SURVEY

MISCELLANEOUS FIELD STUDIES MAP MF – 655J
SHEET 1 OF 2
FOLIO OF THE NABESNA QUADRANGLE, ALASKA

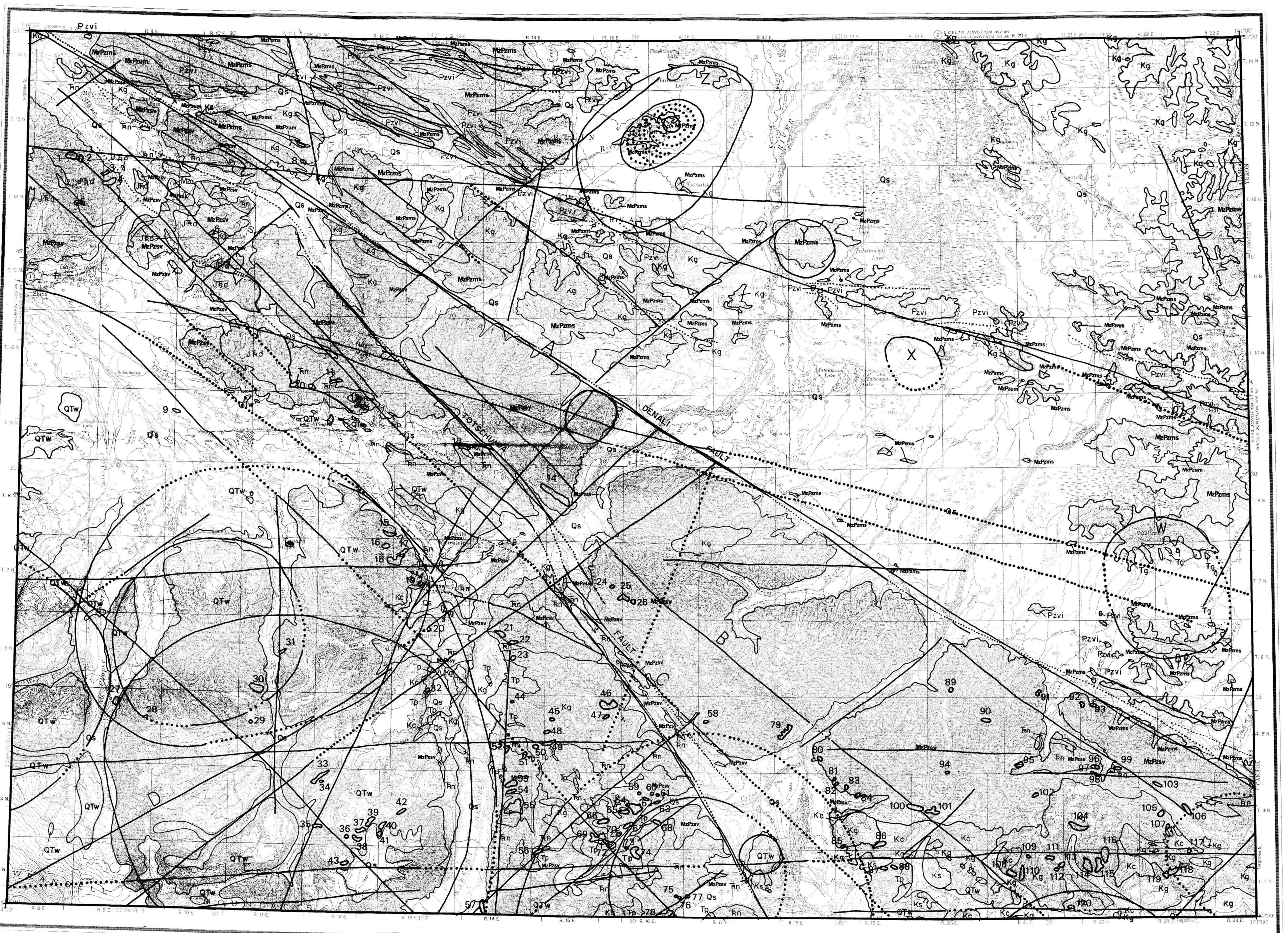

BASE BY U.S. GEOLOGICAL SURVEY, 1960.

TRUE NORTH
MAGNETIC NORTH
APPROXIMATE MEAN DECLINATION, 1962

SCALE 1:250 000
5 0 5 10 15 20 25 MILES
5 0 5 10 15 20 25 KILOMETERS
CONTOUR INTERVAL 200 FEET
DATUM IS MEAN SEA LEVEL

QUADRANGLE LOCATION

Interpretation by N. R. D. Albert, with contributions from E. H. Lathram.

Background information for this folio is published as U.S. Geological Survey Circular 718, available free of charge from the U.S. Geological Survey, Reston, Va. 22092.

EXPLANATION FOR GENERALIZED GEOLOGIC MAP

[Geology generalized from Richter (1975)]

CORRELATION OF MAP UNITS

SURFICIAL DEPOSITS

Qs } QUATERNARY

SEDIMENTARY AND VOLCANIC ROCKS

- QTw } QUATERNARY AND TERTIARY
- Ks } Upper(?) Cretaceous; Kc } Lower Cretaceous } CRETACEOUS
- Ŧn } Upper and(or) Middle Triassic } TRIASSIC
- MzPzsv } MESOZOIC AND PALEOZOIC

INTRUSIVE, METAMORPHIC, AND ULTRAMAFIC ROCKS

- Tp, Tg } TERTIARY
- Kg } CRETACEOUS
- JŦd } JURASSIC AND TRIASSIC
- Mza } MESOZOIC
- MzPzms, MzPzum } MESOZOIC AND PALEOZOIC
- Pzvi } PALEOZOIC

DESCRIPTION OF MAP UNITS

SURFICIAL DEPOSITS

- Qs UNCONSOLIDATED SEDIMENTARY DEPOSITS (Quaternary)

SEDIMENTARY AND VOLCANIC ROCKS

- QTw WRANGELL LAVA (Quaternary and Tertiary)
- Ks CONTINENTAL SEDIMENTARY ROCKS (Upper? Cretaceous)
- Kc CHISANA FORMATION (Lower Cretaceous) Marine and subaerial volcanic rocks
- Ŧn NIKOLAI GREENSTONE (Upper and(or) Middle Triassic)
- MzPzsv UNDIVIDED SEDIMENTARY AND VOLCANIC ROCKS (Mesozoic and Paleozoic)

INTRUSIVE, METAMORPHIC, AND ULTRAMAFIC ROCKS

- Tp PORPHYRY (Tertiary) Porphyritic andesite to rhyodacite
- Tg UNDIVIDED GRANITIC ROCKS (Tertiary) Chiefly quartz monzonite
- Kg UNDIVIDED GRANITIC ROCKS (Cretaceous) Chiefly granodiorite and quartz monzonite
- JŦd DIORITE COMPLEX (Jurassic and Triassic)
- Mza ANORTHOSITE (Mesozoic)
- MzPzms UNDIVIDED METAMORPHOSED SEDIMENTARY ROCKS (Mesozoic and Paleozoic)
- MzPzum UNDIVIDED ULTRAMAFIC ROCKS (Mesozoic and Paleozoic)
- Pzvi UNDIVIDED METAMORPHOSED MAFIC VOLCANIC AND INTRUSIVE ROCKS (Paleozoic)

Contact. Dotted where concealed

Fault. Dotted where concealed

EXPLANATION OF IMAGERY INTERPRETATION

LINEAR FEATURE. DOTTED WHERE UNCERTAIN

CIRCULAR FEATURE. DOTTED WHERE UNCERTAIN

27 COLOR ANOMALY

DISCUSSION

The first Earth Resources Technology Satellite (ERTS-1) was launched by the U.S. National Aeronautics and Space Administration (NASA) on July 23, 1972. (In January, 1975, with the launch by ERTS-2, these satellites were renamed LANDSAT 1 and 2. Because the term ERTS-1 has become so familiar and this study is based entirely on ERTS-1 data, ERTS is used throughout this discussion rather than LANDSAT.) The satellite maintains a near-polar, sun-synchronous orbit at an altitude of approximately 907 km, allowing 14 orbits each day with repeated coverage of the same area every 18 days at the same local solar time.

ERTS-1 contains two imaging systems, the Multispectral Scanner (MSS) and the Return Beam Vidicon (RBV), which record reflected visible and near-infrared radiation. Owing to an electronic malfunction, the RBV system was turned off after about one month of operation. The MSS system, however, has continued to function properly, recording images with high spatial resolution (about 80 m) in four discrete spatially registered spectral bands: band 4, 0.5-0.6 μm; band 5, 0.6-0.7 μm; band 6, 0.7-0.8 μm; band 7, 0.8-1.1 μm. Measurements are transmitted to receiving stations on the ground, and the data are subsequently digitized, calibrated, and converted to pictorial images. Each image covers an area of approximately 185 X 185 km (34,200 km^2). Overlap is 10 percent with preceding and following images and ranges from about 14 percent sidelap at the equator to more than 50 percent sidelap at latitudes greater than 54 degrees.

METHODS OF INTERPRETATION

Analysis of ERTS images can be made by various methods. One is to visually interpret black and white transparencies or prints of individual bands, or false-color composite prints, transparencies, or diazo composites made by optically combining images of several bands. Another method is to use one of several multispectral viewers that optically generate false-color images and are available commercially. All of these techniques, however, have an inherent problem--the inability of photographic materials to reproduce the entire dynamic spectral reflectance ranges of the different bands. To circumvent this problem, computer enhancement techniques may be applied to computer compatible tapes (CCT).

Because reflectance data recorded by the MSS system are digitized before being converted to pictorial images, the entire dynamic reflectance ranges are available on magnetic tape. After application of a system calibration, the dynamic ranges are recorded on tape as digital numbers (DN) ranging from DN 0 to 127 for bands 4, 5, and 6 and from DN 0 to 63 for band 7. CCT's are formatted from these magnetic tapes, and are available from the EROS Data Center, Sioux Falls, South Dakota.

For each MSS scene, four CCT's are required. Each CCT contains data for all four bands covering one-fourth of a scene. Format for each CCT is seven or nine track with 800 bits per inch and odd parity.

For this study of ERTS-1 imagery of the Nabesna quadrangle, Alaska, two techniques were used, the visual study of an ERTS mosaic of Alaska and the study of computer-enhanced ERTS imagery.

The ERTS mosaic of Alaska was constructed in 1973 by the U.S. Department of Agriculture's Soil Conservation Service, using band 7 images generated without computer enhancement. Study of this mosaic was conducted at a scale of 1:1,000,000 and the results transcribed to fit a standard 1:250,000-scale UTM projection map of the Nabesna quadrangle. Because of the synoptic perspective and low sun angle, the mosaic was most useful for identifying linear and circular features and relating them to regional linear and circular patterns. Because the area of the Nabesna quadrangle is completely covered by snow on the Alaska mosaic, tonal variations signifying differences in ground color are not detectable.

For maximum interpretation of surficial spectral reflectance data, three types of computer-enhanced products were generated and studied: (1) standard false color, (2) simulated true color, and (3) color ratio.

On the basis of minimal snow and cloud cover, two ERTS-1 images were selected for computer enhancement: 1692-20150 and 1692-20152. These images were recorded sequentially on June 15, 1974 and overlap about 10 percent. All bands are good quality, although noise caused significant problems on band 6 of both images. Methods for correcting the noise problems of band 6 are discussed subsequently.

CCT's for these two ERTS scenes were processed by the imaging processing facility of the U.S. Geological Survey, Flagstaff, Arizona. The work was directed by Laurence A. Soderblom and Pat S. Chavez. Computer enhancement techniques were applied using a Digital Equipment Corporation, Computer PDP 11/45, yielding computer enhanced CCT's, which were then used in an Optronics Company, Photowrite 1500 System to generate black and white film transparencies. The black and white transparencies were then photographically composited and enlarged, resulting in color transparencies and color prints at 1:250,000 scale.[1/]

Two quarters from each MSS image were selected for processing, giving complete coverage of the Nabesna quadrangle. Corrections for atmospheric effects, sun elevation, noise, and geometric distortions were applied to each quarter.

Effects of atmospheric absorption and scattering can be determined by finding the lowest DN values in the image on a histogram display. These values usually occur over water or in the shadows of clouds. If atmospheric absorption and scattering are significant, the lowest DN values will be somewhat greater than zero. Corrections are then made by subtracting the appropriate DN value for each band from each picture element (pixel).

Because sun elevations and azimuths vary with the time of year, as well as time of day, two images of the same area, taken at different times, will have different illumination. It is, therefore, often desirable to introduce a sun elevation correction to the images, particularly if the images are to be mosaicked. The sun elevation correction applies an illumination approximating a sun elevation of 90 degrees to each image.

Noise patterns in ERTS images are caused by spurious electronic signals, imperfections in the imaging system, and incomplete recalibration of the data. Methods for removing noise are many and varied. However, all methods rely on recognizing erratic or patterned DN values that seem unrelated to details on the earth's surface. Computer techniques reduce or eliminate noise by statistically correcting these erratic or patterned values to the values of pixels selected in some type of geometric array (Chavez, 1975).

The ERTS MSS system is an optical scanning device with six detectors per band and an oscillating mirror. Because of differential motions between the scanning device, the spacecraft, and the rotation of the earth, the data are geometrically distorted with respect to the area of ground covered. These resulting distortions are corrected by computer, giving an image with a parallelogram form and geometric accuracy.

The standard false-color image was produced by compositing bands 4, 5, and 7. After the standard corrections mentioned above, each band was computer filtered to enhance linear and circular features greater than 8.5 pixels in any direction. This information was stored and later added back to the remaining data prior to generation of the actual images. Histograms of the different bands were analyzed and the DN values above and below which no significant amount of data exist were located. These maximum and minimum DN values were then used as limits, and the intervening data were "stretched" (adjusted by computer) to occupy the entire dynamic range of DN values. This stretching technique results in an increase in contrast for each of the bands and ultimately a greater range of colors on the final false-color composite image. Upon completion of computer correction and enhancement techniques, the four quarters--two from each of the two MSS images--were computer mosaicked, forming one scene. An image of each band was then produced as a film positive (transparency) at approximately 1:1,054,000 scale. The transparencies were photographically registered and optically filtered to generate a color transparency at 1:1,054,000 scale. The color used for each band was: band 4, blue; band 5, green; band 7, red (the standard false-color combination). The resulting color product shows vegetation in red, water in black, and snow and clouds in white. Finally, the false-color transparency was photographically enlarged and printed at 1:250,000 scale.

Although bands 4 and 5 measure reflected light in the yellow-green and red-orange regions of the visible spectrum, respectively, bands 6 and 7 measure in the invisible, near-infrared region. Photographically generated color ERTS images, therefore, cannot show actual surficial color conditions. Using computer-enhancement techniques, "simulated" true-color images can be generated, providing a version of ERTS data in which the colors approximate what the human eye should see from orbital altitudes if atmospheric absorption and scattering were eliminated. Briefly, the method involves the prediction and generation of a blue component from the data of the four MSS bands. The final product simulates true color and accentuates subtle color differences. As in the false-color images, the four quarters are mosaicked together and black and white transparencies of bands 4 and 5 and of the extrapolated blue band are produced. In generating the final color products, the three black and white transparencies are optically filtered using green for band 4, red for band 5 and blue for the synthetic blue band (Eliason and others, 1974).

The third type of computer-enhanced product was a color ratioed image. Ratioing involves dividing the DN values of pixels in one spectral band by the DN value of the same pixels in another spectral band. The resulting image tends to eliminate variations in color of a given material due to topographic effects or shadows. On the other hand, differences in albedo are reduced and different materials, easily discriminated on a standard photographic image, may become visually identical or similar. Histograms of ratioed images tend to have a narrow range of DN values. As a result, contrast stretching is used to fill the entire dynamic range of values, giving greater variations in color. The type of stretch is dependent upon the brightness of the area of interest. Effects of noise and atmosphere are greatly enhanced by ratioing, requiring extra care in the early computer processing stages. For this study the ratios were as follows: band 5/4, band 6/4, band 4/5. The quotients were converted into black and white transparencies that were composited into the final color products, using red for 5/4, green for 6/4, and blue for 4/5.

RESULTS

As stated above, the most useful application of the 1:1,000,000-scale Alaskan ERTS mosaic prepared by the Soil Conservation Service was the identification of linear and circular features. These features were traced onto a scale-stable plastic overlay, then photographically enlarged to a scale of 1:250,000. Because of optical distortions and differences in projections (the mosaic is Albers Equal Area, and the map, Universal Transverse Mercator) the final locations of the various linears and circulars are accurate to within only about 1 km. This is not a significant problem, however, since most linear and circular features appear to be zones, many of which are wider than 1 km.

Linear Features

Linears more than 10 km long were plotted. Shorter linears are too numerous to plot and would virtually fill any diagram showing them all. The longest linear observed corresponds to the Denali fault trace and exceeds 185 km in length.

Three nearly orthogonal sets of linears are evident in areas south of the Denali fault. The predominant set trends approximately N.43W. and N.48E., while the other sets trend approximately N.72W. and N.20E. and about N.87E. and north. Northwest-, northeast-, and east- trending linears exhibit a spatial periodicity. Parallel linears with any of these trends tend to be spaced approximately 35 km apart. This phenomenon is pronounced in the Nabesna quadrangle south of the Denali fault and in the McCarthy quadrangle.

Although linears are less common in the part of the Nabesna quadrangle north of the Denali fault, the predominant N.43W.-N.48E. orthogonal set seems to be uninterrupted across the fault. Just north of the Nabesna quadrangle, linear patterns observed in lowland lake areas very nearly parallel not only the N.43W.-N.48E. set but also the N.72W.-N.20E. set (Lathram and Albert, 1975). This suggest that, although the Denali fault is a major geologic and tectonic structural break, the origin of the regional linear patterns may be independent of the forces causing recorded activity along the Denali fault.

Close scrutiny of the Alaska mosaic reveals that from the northernmost part of the Alaska Range, where the Denali fault forms an arc and curves southwestward, a subtle continuation of linear A extends northwest to Kotzebue Sound (see index map). To the southeast, linear A continues east of the Coast Range in British Columbia, on strike with Campbell's (1972) northwestward extension of the Fraser-Yalakom fault system, suggesting that the Denali fault may not be deflected southward to join with the Chatham Strait fault (Lathram and Albert, 1975).

Both linears B and C appear to extend more than 700 km. Linear B can be traced from approximately the central part of the Nabesna quadrangle to near Tracy Arm, southeastern Alaska. Linear C appears to extend from an area in the northernmost part of the Alaska Range to Seymour Canal, southeastern Alaska.

Northeast-trending linears appear to be less continuous than those trending northwest. Most appear to terminate near or at the Denali fault. The most well developed, D, can be traced from Prince William Sound in the southwest to the Denali fault, with a minor break in continuity in the northern part of the Wrangell Mountains.

The east-trending linears are also locally discontinuous. Linear E, although not discernible in the lowland area between the Wrangell Mountains and the Talkeetna Mountains, seems to be in line with the trace of the Castle Mountain fault, south of the Talkeetna Mountains. To the northeast, this linear crosses the Denali fault, becoming discontinuous and ending some tens of kilometres east of the border between Alaska and the Yukon Territory, Canada. Aeromagnetic data (Griscom, 1975) and gravity data (Barnes and Morin, 1975) suggest the existence of major east-trending structural control by some as yet unknown tectonic feature(s) in the southern part of the Nabesna quadrangle. East-trending linears are more common in the southern parts of the Nabesna quadrangle and may be expressions of the observed east-trending geophysical anomalies. The known metallic mineral occurrences also are more common in the southern part of the Nabesna quadrangle, suggesting that they may be related to these east-trending structures.

The nature of the linears observed on the Alaskan ERTS mosaic and their significance in mineral resource evaluation are poorly understood. Previous studies (Lathram and Albert, 1975) suggest that linears can be divided into three main groups on the basis of length: 10 to about 200 km, about 200 km to 1,000 km, and >1,000 km. Shorter linears tend to be more abundant and varied in trend and appear to be related to more recent tectonic features. Longer linears are less abundant and less varied in trend and reflect older, more deeply buried structures, possibly crustal fractures.

A relation between "giant" (>1,000 km) northwest- and northeast- trending linears and the occurrence of mineral deposits has been postulated by Lathram and Gryc (1973). In the Nabesna quadrangle approximately 56 percent of the known mineral deposits occur on or within about 1 km of linears more than 10 km long. The correlation of known mineral deposits with "giant" linears, however, is poor, suggesting that the relation proposed by Lathram and Gryc may apply to much larger mineralized regions and may not be recognizable at the scale of a single quadrangle. Nevertheless, the observed correlation between known mineral deposits and linears in the Nabesna quadrangle seems more than fortuitous and may reflect a genetic relation.

Circular Features

Circular features more than 5 km in diameter were plotted in this study. Larger circular features are abundant in the Wrangell Mountains south of the Denali fault. The largest is a circular feature more than 200 km in diameter, part of which lies in the western part of the Nabesna quadrangle.

The volcanic nature of the Wrangell Mountains, and the clustering of circular features in areas of volcanoes, suggests that many of these circular features may be the surficial expressions of magma chambers that have caused doming or have collapsed. Considerably more data are needed, however, to relate these circular features more specifically to crustal or subcrustal activities.

North of the Denali fault are four circular features that appear to be unrelated to Cenozoic volcanic activity. Circular feature W occurs in the Wellesley Mountain-Carden Hills area and is approximately 15 km to 20 km in diameter. The origin of this circular feature may be associated with the intrusion of the Snag Creek pluton of Tertiary age (Richter, 1975). The outline of the circular feature may define the areal extent of the buried intrusive body.

Circular feature X was located on the computer enhanced, false-color composite as a weak color anomaly in the lowland area south of the Black Hills. The area is covered with alluvial and glacial deposits of Quaternary age. Aeromagnetic data, however, show a magnetic low in the area where the circular feature is best defined, suggesting the possibility of a hidden felsic (magnetite-poor) intrusive body. The observed circular feature is about 5 km to 7 km in diameter, but the aeromagnetic data suggest a somewhat smaller body.

Circular feature Y occurs in the hilly region between Mundthag Lake and the Nabesna River and is about 6 km in diameter. The region is mostly covered by Quaternary alluvium, colluvium, and eolian and glacial deposits overlying metamorphosed Devonian marine sedimentary rocks intruded by small Cretaceous diorite-gabbro plutons (Richter, 1975). Although the metamorphosed Devonian rocks are not confined to this area, they crop out in a circular pattern that corresponds closely to the outline of the observed circular feature. In addition, aeromagnetic data (Griscom, 1975) show a pronounced contour deflection and a magnetic high corresponding to the circular feature and the outcrop pattern of the Devonian rocks. Griscom interprets the magnetic anomaly as a contact metamorphic aureole, but these correlations may also suggest doming in the area, possibly due to a hidden intrusive body associated with the numerous small diorite-gabbro bodies that intrude the Devonian metamorphic rocks.

Circular feature Z was identified on the computer-enhanced, false-color composite and appears to be a series of subtle concentric elliptical features, the largest of which has dimensions of about 17 km and 25 km. The next largest concentric ellipse has dimensions of about 7 km and 10 km, outlining Kinshuda Hill. Numerous other more poorly defined concentric ellipses occur within the Kinshuda Hill area. The rocks are predominantly Devonian greenstone and Paleozoic metamorphosed volcanic and intrusive rocks with peripheral metamorphosed marine sedimentary rocks of Devonian age. Aeromagnetic data reveal a significant contour deflection and general high for the area. Unlike circular feature Y, the magnetic contour outlines do not correspond very closely to the circular features. The contours do suggest, however, that control of the deflections and high magnetic regime may be related to the formation of the concentric circular features and to a hidden body to which the Paleozoic intrusive rocks may be related.

The results of this study do not show a clear genetic relation between circular features and mineral deposits in the Nabesna quadrangle. In the Wrangell Mountains area, where the circular features are most common, there are only a few known mineral occurrences. However, large areas are covered by Cenozoic volcanic rocks, and data that might suggest correlations between mineral occurrences and circular features are lacking. On the other hand, in areas such as those north of the Denali fault, information on circular features observed on ERTS imagery along with geophysical and surficial geological information could reveal buried structures or intrusive bodies with which exploitable mineral occurrences might be associated.

Table 1.--*Correlation of color anomalies with geologic and geophysical data*

Anomaly number	Simulated true color	False color	Geologic map unit and symbol (Richter, 1975)	Coincident aeromagnetic anomaly (Griscom, 1975)	Proximity to and trend of linear feature	Type of coincident known mineral occurrence (Richter, Singer, and Cox, 1975)	Probable cause of anomaly (Richter, oral commun., 1975)
1		Pale green	Diorite complex (JŦd, JŦg)		On NW, near E		Alteration in diorite and quartz diorite
2		Pale green	Diorite complex (JŦd, JŦg)		On NW	Gossan	Alteration in diorite and quartz diorite
3		Pale green	Diorite complex (JŦs)		Near NW		Alteration in cataclasite
4		Pale green	Diorite complex (JŦs)		On NW		Alteration in cataclasite
5		Grayish yellow	Tetelna Volcanics (P ℙt)		Near NW	Near gossan	Alteration in volcanic rocks
6		Grayish yellow	Limestone (Ŧl)		On NW		Limestone
7		Pale green	Ultramafic rocks (Kum)		Near N		Silica carbonate rock and ultramafic rock
8	Light brown	Grayish yellow	Tok-Tetlin pluton (Kmg)		Near E		Alteration in quartz monzonite
9	Moderate reddish orange		Glacial deposits (Qwg) Alluvial deposits (Qau)		Near NW		Unknown
10	Grayish yellow		Nikolai Greenstone (Ŧn) Limestone (Ŧl)				Limestone
11	Grayish green	Moderate yellow	Nikolai Greenstone (Ŧn) Limestone (Ŧl)		Near NW	Pb, Ag; gossan	Alteration in limestone
12	Yellowish gray		Nikolai Greenstone (Ŧn) Limestone (Ŧl)		Near NW		Limestone
13	Moderate greenish yellow		Nikolai Greenstone (Ŧn) Limestone (Ŧl)			Near Cu	Limestone
14	Dusky yellow	Light green	Marine sedimentary rocks (KJs)		Near NE		Alteration of iron carbonate-bearing siltstone
15	Pale greenish yellow		Wrangell Lava (QTwr)		Near NW		Rhyolite dome
16		Pale green	Wrangell Lava (QTwr)				Palagonitic tuff breccia
17	Pale greenish yellow	Pale green	Wrangell Lava (QTwr)				Rhyodacite dome
18	Pale green		Wrangell Lava (QTwr, QTw)	High	Near E		Rhyodacite dome
19	Very pale green		Marine sedimentary rocks (KJs) Undifferentiated diorite (TKd) Limestone (Ŧl)	High	On NE	Cu,Au,Pb,Ag,Zn	Alteration in quartz diorite
20		Light blue green	Chisana Formation (Kc)		On NE	Gossan	Alteration in volcanic rocks
21	Pale yellowish green		Limestone (Ŧl) Nikolai Greenstone (Ŧn)		Near NE		Limestone
22	Pale yellowish green		Limestone (Ŧl) Nikolai Greenstone (Ŧn)	High	Near N		Alteration in porphyry and limestone
23	Pale yellowish green		Nabesna pluton (Kng) Nikolai Greenstone (Ŧn)		Near N	Near gossan	Alteration zone
24	Light olive brown	Light green	Marine sedimentary rocks (KJs)				Alteration of iron carbonate-bearing marine sedimentary rocks
25	Light olive gray	Light green	Marine sedimentary rocks (KJs)				Alteration of iron carbonate-bearing marine sedimentary rocks
26	Light olive gray	Light green	Marine sedimentary rocks (KJs)				Alteration of iron carbonate-bearing marine sedimentary rocks
27	Dusky yellow		Anomalously colored lake	No data			Glacial silt-filled lake
28	Dark yellowish orange	Moderate yellow	Wrangell Lava (Qw)	No data			Dacite flow breccia
29	Moderate reddish orange		Colluvial deposits (Qc) Wrangell Lava (QTw)				Rhyolite dome
30	Grayish green	Pale green	Wrangell Lava (QTw)	High-low pair			Unknown
31		Pale green	Wrangell Lava (QTw)		On N		Unknown
32		Moderate greenish yellow	Chisana Formation (Kc)		Near NE		Alteration in volcanic rocks
33	Grayish yellow green	Moderate yellowish green	Wrangell Lava (Qw)				Palagonitic airfall tuffs
34	Grayish yellow green	Moderate yellowish green	Wrangell Lava (QTw)				Unknown
35	Grayish yellow green		Wrangell Lava (Qw)	No data	On NE, near NW		Palagonitic airfall tuffs
36		Moderate yellowish brown	Wrangell Lava (Qw)		Near NW		Palagonitic airfall tuffs
37		Dark greenish yellow	Wrangell Lava (Qw)				Palagonitic airfall tuffs
38		Moderate greenish yellow	Wrangell Lava (Qw)				Palagonitic airfall tuffs
39		Dark greenish yellow	Wrangell Lava (Qw) Alluvial deposits (Qau)				Palagonitic airfall tuffs
40		Dark greenish yellow	Wrangell Lava (Qw)				Palagonitic airfall tuffs
41		Dark greenish yellow	Wrangell Lava (Qw)				Palagonitic airfall tuffs
42	Very dark red & very pale green	Moderate yellowish green	Wrangell Lava (Qw)				Palagonitic airfall tuffs
43		Moderate greenish yellow	Wrangell Lava (Qw) Colluvial deposits (Qc)	No data	Near E		Palagonitic airfall tuffs
44	Very pale green		Nabesna pluton (Kng)		Near N		Alteration in granodiorite
45	Pale yellowish green		Nabesna pluton (Kng)			Near Cu, Mo; gossan	Alteration in granodiorite
46		Moderate greenish yellow	Nabesna pluton (Kng) Glacial deposits (Qag)		Near NE		Unknown
47		Moderate greenish yellow	Nabesna pluton (Kng)		Near NE		Unknown
48	Pale greenish yellow		Nabesna pluton (Kng) Colluvial deposits (Qc) Younger porphyry (Tp)		Near E	Near Pb,Mo,Zn,Cu,Au; gossans	Alterations associated with Bond Creek Cu porphyry
49		Moderate yellowish green	Tetelna Volcanics (P ℙt) Nikolai Greenstone (Kng)		On E	Pb,Mo,Zn,Cu,Au; gossan	Alterations associated with Bond Creek Cu porphyry
50	Dark yellowish orange		Tetelna Volcanics (P ℙt)		Near E	Near Pb,Mo,Zn,Cu,Au; gossan	Alterations associated with Bond Creek Cu porphyry
51	Dark yellowish orange		Tetelna Volcanics (P ℙt) Eagle Creek Formation (Pe, Pel)		On NW	Pb; gossan	Alteration in breccia pipe
52	Pale yellowish green		Tetelna Volcanics (P ℙt) Eagle Creek Formation (Pel, Pe)		On N, near E	Cu,Au,Mo,Ag,Zn; gossan	Alteration in quartz plagioclase porphyry
53	Pale yellowish green		Tetelna Volcanics (P ℙt) Eagle Creek Formation (Pel, Pe)		Near N	Cu; near gossan	Alteration in volcanic rocks
54	Pale yellowish green		Eagle Creek Formation (Pe, Pel) Younger porphyry (Tp)		Near N	Near Cu	Alteration in volcanic rocks
55	Pale yellowish green		Younger porphyry (Tp)	Low	Near N	Near Cu and Zn; near gossan	Alteration in porphyry
56		Dark greenish yellow	Younger porphyry (Tp) Glacial deposits (Qag)	Low	On NE		Alteration in porphyry
57	Grayish orange		Alluvial deposits (Qa, Qau)		On NE		Heavily silted stream
58		Yellowish gray	Marine sedimentary rocks (KJs)		Near NE & NW		Unknown
59	Dark yellowish orange		Tetelna Volcanics (P ℙt) Eagle Creek Formation (Pel)				Alteration of porphyry and contact zones with volcanic rocks
60	Light green		Tetelna Volcanics (P ℙt)				Alteration of porphyry and contact zones with volcanic rocks
61	Light green		Tetelna Volcanics (P ℙt)				Alteration of porphyry and contact zones with volcanic rocks
62	Grayish yellow		Tetelna Volcanics (P ℙt)				Alteration of porphyry and contact zones with volcanic rocks
63	Pale greenish yellow		Younger porphyry (Tp)				Alteration of porphyry and contact zones with volcanic rocks
64		Light green	Tetelna Volcanics (P ℙt) Eagle Creek Formation (Pel, Pe)				Alteration of porphyry and contact zones with volcanic rocks
65	Pale yellowish green	Light green	Tetelna Volcanics (P ℙt)				Alteration of porphyry and contact zones with volcanic rocks
66	Moderate greenish yellow	Dark greenish yellow	Eagle Creek Formation (Pel)		Near NW		Alteration of porphyry and contact zone with volcanic rocks
67	Pale yellowish green		Colluvial deposits (Qc)	Low			Alteration of porphyry and contact zone with volcanic rocks
68	Pale yellowish green		Eagle Creek Formation (Pe, Pel) Tetelna Volcanics (P ℙt)		On NE		Alteration of porphyry and contact zone with volcanic rocks
69		Dark greenish yellow	Younger porphyry (Tp) Eagle Creek Formation (Pel) Tetelna Volcanics (P ℙt)		On NW	Pb, Ag, Zn; gossan	Alteration in breccia pipe
70	Pale yellowish green		Glacial deposits (Qag) Younger porphyry (Tp)				Alteration of porphyry and contact zones with volcanic rocks
71	Light green		Younger porphyry (Tp) Tetelna Volcanics (P ℙt)		On NW	Near Pb, Ag, Zn; near gossan	Alteration of porphyry and contact zones with volcanic rocks
72	Pale yellowish green		Glacial deposits (Qag) Younger porphyry (Tp) Tetelna Volcanics (P ℙt)		Near NW	Near Cu (?)	Alteration of porphyry and contact zones with volcanic rocks
73	Light green		Younger porphyry (Tp)		Near NE		Alteration of porphyry and contact zones with volcanic rocks
74	Grayish orange	Light green	Younger porphyry (Tp) Tetelna Volcanics (P ℙt) Eagle Creek Formation (Pel, Pe)		Near NE		Alteration of porphyry and contact zones with volcanic rocks
75	Pale green	Moderate yellowish green	Nikolai Greenstone (Ŧn)		Near NE		Unknown
76	Dark yellowish orange		Nikolai Greenstone (Ŧn)		Near NE		Unknown
77	Moderate reddish brown		Nikolai Greenstone (Ŧn)		On NE		Unknown
78		Moderate yellowish green	Nikolai Greenstone (Ŧn)		NE and NW		Unknown
79		Grayish yellow	Marine sedimentary rocks (KJs) Colluvial deposits (Qc)				Unknown
80		Light green	Marine sedimentary rocks (KJs)				Alteration along covered thrust fault zone in marine sedimentary rocks
81		Grayish yellow	Marine sedimentary rocks (KJs)				Alteration along covered thrust fault zone in marine sedimentary rocks
82		Grayish yellow	Marine sedimentary rocks (KJs)				Alteration along covered thrust fault zone in marine sedimentary rocks
83		Grayish yellow	Marine sedimentary rocks (KJs)				Alteration along covered thrust fault zone in marine sedimentary rocks
84		Grayish yellow	Marine sedimentary rocks (KJs) Rock glacier deposits (Qr)			Near Au placer	Alteration along covered thrust fault zone in marine sedimentary rocks
85		Moderate pink	Chisana pluton (Kcs)			Near gossan	Alteration in syenodiorite
86		Light green	Chisana Formation (Kc) Chisana pluton (Kcs)			Cu, Au, near Au placer; gossan	Alteration in contact zone of syenodiorite
87	Yellowish gray		Wrangell Lava (QTwr) Colluvial deposits (Qc)		Near E	In general Au placer area	Rhyolite domes
88	Yellowish gray		Wrangell Lava (QTwr) Chisana Formation (Kc)		Near E	In general Au placer area	Rhyolite domes
89		Moderate orange pink	Marine sedimentary rocks (KJs)				Unknown
90		Yellowish gray	Marine sedimentary rocks (KJs)				Unknown
91		Grayish yellow	Marine sedimenatry rocks (KJs)				Unknown
92		Grayish orange	Marine sedimentary rocks (KJs)				Unknown
93		Moderate greenish yellow	Marine sedimentary rocks (KJs) Colluvial deposits (Qc)		Near NW		Unknown
94	Moderate yellow		Marine sedimentary rocks (KJs)				Unknown
95		Moderate yellowish green	Marine sedimentary rocks (KJs) Limestone (Ŧl) Nikolai Greenstone (Ŧn)		Near E		Limestone
96	Yellowish gray		Limestone (Ŧl) Colluvial deposits (Qc)?		Near E		Limestone
97	Light brown		Limestone (Ŧl)		On E		Limestone or alteration in porphyry
98	Grayish yellow		Nikolai Greenstone (Ŧn) Marine sedimentary rocks (KJs)		On E		Limestone or alteration in porphyry
99	Grayish yellow		Nikolai Greenstone (Ŧn)		Near NW		Limestone
100	Yellowish gray	Light green	Marine sedimentary rocks (KJs) Colluvial deposits (Qc)		On NW	Near Au placers	Alteration in large thrust fault zone
101	Yellowish gray	Light green	Marine sedimentary rocks (KJs) Colluvial deposits (Qc)		Near NW	Near Au placers	Alteration in large thrust fault zone
102		Moderate yellowish green	Marine sedimentary rocks (KJs) Klein Creek pluton (Kkg)			Gossan	Alteration in diorite and marine sedimentary rocks
103	Moderate yellowish green		Limestone (Ŧl) Marine sedimentary rocks (KJs) Eagle Creek Formation (Pe)		Near NW & E		Limestone
104		Pale green	Klein Creek pluton (Kkg) Rock glacier deposits (Qr) Glacial deposits (Qag)			Gossan	Alteration in quartz monzonite
105	Pale yellowish green		Klein Creek pluton (Kkd)			Near gossan	Alteration in mafic diorite
106		Light green	Tetelna Volcanics (P ℙt) Undifferentiated diorite (TKd)		On NW	Gossan	Alteration in volcanic rocks
107	Dusky yellow	Moderate yellowish green	Klein Creek pluton (Kkd)			Gossan	Alteration of Baultoff Cu porphyry
108	Pale greenish yellow	Pale green	Klein Creek pluton (Kkg) Chisana Formation (Kc)		Near NW	Cu, Mo; gossan	Alteration of Garl Creek Cu porphyry
109	Moderate yellowish green	Pale green	Klein Creek pluton (Kkg) Colluvial deposits (Qc)		On E	Near gossan	Alteration of granodiorite
110		Pale green	Klein Creek pluton (Kkg)	Low		Cu, Mo; near gossan	Alteration of Carl Creek Cu porphyry
111		Pale green	Klein Creek pluton (Kkg)		Near E		Unknown
112		Pale green	Klein Creek pluton (Kkg)				Unknown
113		Pale green	Klein Creek pluton (Kkg)	High	Near E		Unknown
114		Pale green	Klein Creek pluton (Kkg) Colluvial deposits (Qc)		Near E		Unknown
115		Pale green	Klein Creek pluton (Kkg) Colluvial deposits (Qc)		Near E		Unknown
116		Pale green	Klein Creek pluton (Kkg) Colluvial deposits (Qc)	Low	On E		
117	Moderate yellowish green		Chisana Formation (Kc) Continental sedimentary rocks (Ks)		Near E	Near Cu, Pb	Alteration along thrust fault
118	Grayish blue green		Marine sedimentary rocks (KJs) Klein Creek pluton (Kkg)			Cu; gossan	Alteration of Horsfeld Cu porphyry
119		Light green	Klein Creek pluton (Kkg) Marine sedimentary rocks (KJs)			Cu; gossan	Alteration of Horsfeld Cu porphyry
120	Yellowish gray		Chisana Formation (Kc)		Near E	Gossan	Alteration in volcanic rocks

Color Anomalies

Interpretation of computer-enhanced ERTS imagery--false color, simulated true color and color ratio--primarily involved the identification of color anomalies, nearly all of which were in areas of little or no vegetation or snow cover. A color anomaly is considered to be a variation in tone or color observed on ERTS imagery that differs significantly from the general local background color, indicating a reflectivity difference on the ground. The anomalies were subsequently assigned a number, tabulated, and correlated with other information (table 1).

Color terms used to describe the anomalies are those on the Rock-color Chart distributed by the Geological Society of America. Since color anomalies in any area are actually made up of numerous pixels of different colors, the color assigned to each anomaly represents an average macroscopic color impression.

Color anomalies were most pronounced on the false-color and simulated true-color images. Mountainous areas with little or no vegetation tended to have virtually no significant color variations on the color ratio product. Instead, lowland areas with heavy vegetative cover showed the greatest variety of colors, owing to the computer stretching technique used after the ratioing was completed. Time limitations prohibited the programming of a different stretch to enhance vegetation-free areas. As a result no color anomalies were identified on the color ratio image. However, using computer ratioing techniques, Rowan and others (1974) were able successfully to detect and map hydrothermally altered areas and to discriminate most major rock types in south-central Nevada, indicating that these techniques can have important applications to mineral resource exploration and regional geologic mapping.

Generally, anomalies in the same rock unit tend to be of similar color and commonly tend to show up in either one or the other color image, but not both. For example, anomalies in the Klein Creek pluton (Richter, 1975) tend to be pale green in the false-color image, yet are rarely seen in the simulated true-color image.

Correlation of color anomalies with aeromagnetic data (Griscom, 1975) was poor. Only ten anomalies were found to correspond to areas of magnetic highs or lows. Interpretations as to the significance of these relations require further study.

Correlation of color anomalies with linears was good; 58 percent of the observed color anomalies occur on or within 1 km of a linear. Given the location inaccuracies for linears (as described earlier), 1-km proximity is probably statistically significant.

Correlation of color anomalies with known mineral occurrences (Richter and others, 1975) was fair. Approximately 32 percent of the observed color anomalies occur within 1 km of known metallic mineral occurrences or mapped gossans, and about 34 percent of the known metallic mineral occurrences occur within 1 km of observed color anomalies. Information relating color anomalies observed on ERTS imagery to probable geologic causes was supplied by D. H. Richter (oral commun., 1975) and shows a striking correlation between color anomalies and areas of alteration on the ground. About 55 percent of the observed color anomalies correspond to altered zones and 25 percent correspond to various other geologic phenomena. The remaining 20 percent are unexplained. Thus, 70 percent of the explained color anomalies are related to altered zones.

Correlation of known mineral occurrences and associated observed color anomalies with linears was excellent. Approximately 70 percent of the observed color anomalies that correspond to known metallic mineral occurrences or mapped gossans occur within 1 km of a linear. Also, about 78 percent of the known mineral occurrences that correspond to observed color anomalies occur within 1 km of a linear.

Complete information on geochemical data are not available to date. However, preliminary data suggest a good correlation between color anomalies and areas of high geochemical anomalies (D. A. Singer, oral commun., 1975).

CONCLUSIONS

Many mineralized areas in the Nabesna quadrangle can be detected by computer-enhanced ERTS imagery and many areas that show color anomalies associated with linears may have a high potential for metallic mineral occurrence. The existence of significant new metallic mineral occurrences in the Nabesna quadrangle cannot at this time be determined by ERTS imagery alone, but about 20 percent of the observed color anomalies remain unexplained, some possibly indicating sites for mineral exploration. Additional information as to the actual causes of the color anomalies observed on ERTS images in this study is necessary in order to improve interpretative techniques. Nevertheless, correlations of ERTS data with geophysics, geochemistry, and geology promise to be useful in mineral exploration or in a mineral assessment program.

REFERENCES CITED

Barnes, D. F., and Morin, R. L., 1975, Gravity map of the Nabesna quadrangle, Alaska: U.S. Geol. Survey Misc. Field Studies Map MF-655-I, 1 sheet, scale 1:250,000.

Campbell, D. D., 1972, Regional faults and the Bridge River gold deposits (abs.), in Program and abstracts, Symposium on faults, fractures and lineaments and related mineralization in the Canadian Cordillera, Vancouver, B. C., Feb.,1972: Vancouver, B. C., Geol. Assoc. Canada, Cordilleran Sec., p. 16.

Chavez, P. S., Jr., 1975, Simple high-speed digital image processing to remove quasi-coherent noise patterns: Proceedings, American Society of Photogrammetry and American Congress on Surveying and Mapping Conference, Mar. 9-19, 1975, Washington, D. C. (in press).

Eliason, E. M., Chavez, P. S., and Soderblom, L. A., 1974, Simulated "true color" images from ERTS data: Geology, v. 2, no. 5, p. 231-234.

Griscom, Andrew, 1975, Aeromagnetic map and interpretation of the Nabesna quadrangle, Alaska: U.S. Geol. Survey Misc. Field Studies Map MF-655-H, 2 sheets, scale 1:250,000.

Lathram, E. H., and Albert, N. R., 1975, Significance of space image linears in Alaska: Proceedings, First International Conference on the New Basement Tectonics, June 3-7, 1974, Utah Geol. Soc., Salt Lake City, Utah, 35 p. (in press).

Lathram, E. H., and Gryc, George, 1973, Metallogenic significance of Alaskan geostructures seen from space: Proceedings, Eighth Internat. Symposium on Remote Sensing of Environment, Environmental Research Institute of Michigan, Ann Arbor, Mich., p. 1209-1211.

Richter, D. H., 1975, Geologic map of the Nabesna quadrangle, Alaska: U.S. Geol. Survey Misc. Field Studies Map MF-655-A, 1 sheet, scale 1:250,000.

Richter, D. H., Singer, D. A., and Cox, D. P., 1975, Mineral resources map of the Nabesna quadrangle, Alaska: U.S. Geol. Survey Misc. Field Studies Map MF-655-K, 1 sheet, scale 1:250,000.

Rowan, L. C., Wetlaufer, P. H., Goetz, A. F. H., Billingsley, F. C., and Stewart, J. H., 1974, Discrimination of rock types and detection of hydrothermally altered areas in south-central Nevada by the use of computer-enhanced ERTS images: U.S. Geol. Survey Prof. Paper 883, 35 p.

[1/] Computer-enhanced color products and enhanced computer compatible tapes, generated by the U.S. Geological Survey, Flagstaff, Arizona, are available, at nominal cost, from: Alaskan Technical Data Unit, U.S. Geological Survey, 345 Middlefield Road, Menlo Park, Calif. 94025.

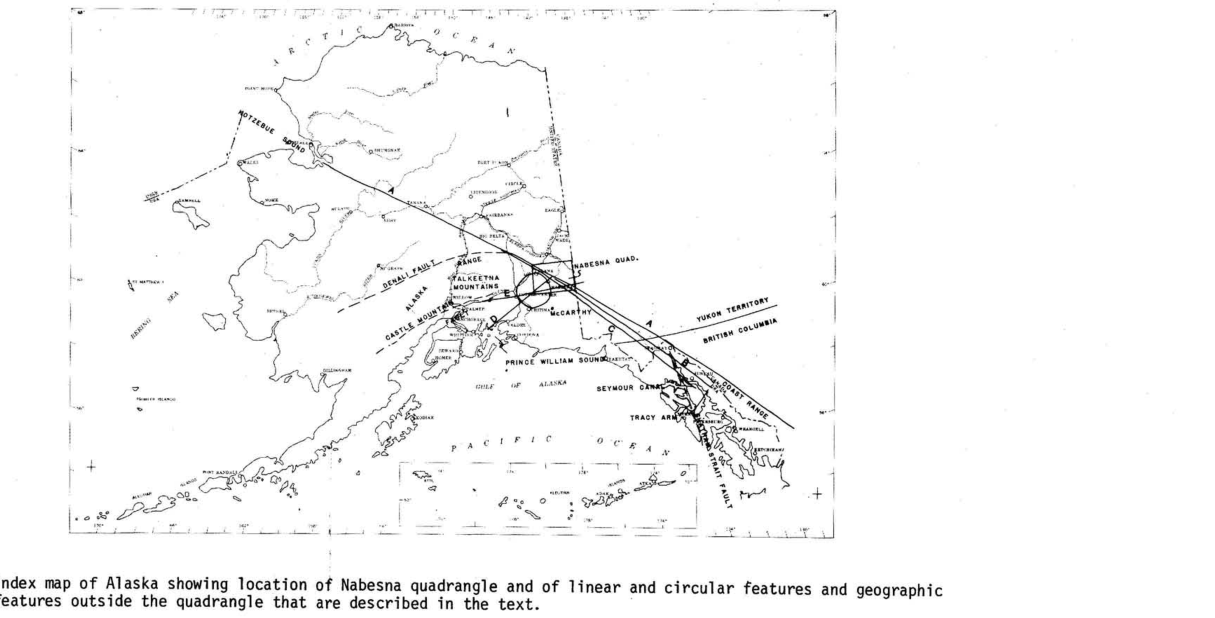

Index map of Alaska showing location of Nabesna quadrangle and of linear and circular features and geographic features outside the quadrangle that are described in the text.

INTERPRETATION OF EARTH RESOURCES TECHNOLOGY SATELLITE IMAGERY OF THE NABESNA QUADRANGLE, ALASKA

BY

NAIRN R. D. ALBERT

1975

For sale by U. S. Geological Survey, price $1.00 per set